TECHNICAL PHYSICS LETTERS

Founded by Ioffe Institute

Published since January 1975, 12 issues annyally

ISSN: 1063-7850 (print), 1090-6533 (online)

TECHNICAL PHYSICS LETTERS is the English translation of ПИСЬМА В ЖУРНАЛ ТЕХНИЧЕСКОЙ ФИЗИКИ (PIS'MA V ZHURNAL TEKHNICHESKOI FIZIKI)

Published by Ioffe Institute

Saint Petersburg
Ioffe Institute

05

The influence of geometry on spin wave propagation in a system of two waveguiding structures with linearly varying width

© V.A. Gubanov[1], F.E. Garanin[1], A.V. Ognev[2], A.V. Sadovnikov[1]

[1] Saratov National Research State University, Saratov, Russia
[2] Sakhalin State University, Yuzhno-Sakhalinsk, Russia
E-mail: vladmeen@gmail.com

Received May 29, 2025
Revised August 18, 2025
Accepted August 29, 2025

A study of the influence of geometry on spin wave propagation has been carried out using micromagnetic simulations in a composite waveguide structure made of Iron-Yttrium Garnet film with linearly varying widths. It is shown that increasing the distance between waveguides with linearly varying widths leads to a reduction in the frequency bandwidth due to the cutoff of the high-frequency region. The structure can be used as a spatial and frequency filter.

Keywords: spin waves, magnonics, linear change of direction, multiport structure, waveguide system.

DOI: 10.61011/TPL.2026.01.62808.20391

The physics of excitation and transmission of spin waves (SWs) has attracted much recent research attention. The production of magnonic devices [1] will open up an alternative path to the development of logical elements and expand the range of available instruments. The main difference between magnonic and semiconductor devices is that data is transferred not through the propagation of electrons, which is accompanied by the release of Joule heat, but through the precession of magnetization of electron spins, which are fixed in the crystal lattice of the material [2–4]. Ferro- and ferrimagnetic materials are used in this case.

One candidate component for devices based on magnonic principles are yttrium iron garnet (YIG) films, which are characterized by an extremely small constant of SW damping [5–9]. Various methods may be used to synthesize YIG films. One of them is liquid-phase epitaxy, which provides an opportunity to form films with a thickness of $1-10\,\mu$m. This method attracts particular attention due to the potential to synthesize films with a ferromagnetic resonance width of ~ 0.5 Oe at a frequency of 9.7 GHz.

YIG films allow one to fabricate structures of various geometries: planar waveguides, systems of waveguides on a single substrate, structures with a varying direction of the group velocity of SWs (curved structures) [10,11], and periodic structures with a non-uniform thickness [12].

A structure with a linearly varying width was used in [13] for short-wavelength excitation. An increase in group velocity in the process of SW propagation was observed in the structure with a linearly varying width examined in [14].

If magnonic waveguides of the same width are located close to each other, spin-wave coupling establishes periodic energy transfer between the waveguides [15] via the dipole interaction of two laterally adjacent magnetic stripes. The geometry investigated here is more complex and is distinguished from the above systems by a linearly varying waveguide width. The novelty of our work lies in identifying the influence of the width gradient on the conditions and efficiency of coupling between waveguides.

In the present study, micromagnetic modeling in MuMax^3 [16] is used to reveal the regimes of SW propagation in the structure of waveguides with linearly varying widths separated by a gap. The influence of the gap parameter on the characteristics of spin-wave propagation and the regimes of redistribution of spin-wave power to the output channels is demonstrated.

The structure under study is a system of laterally coupled waveguides (two waveguides with widths varying along the entire structure; see Fig. 1). These waveguides are YIG films with thickness $t = 10\,\mu$m, which were formed in experiments on a gadolinium gallium garnet substrate by liquid-phase epitaxy. These coupled waveguides had the following parameters: structure length $L_0 = 7000\,\mu$m, width of the larger part of the trapezoid $w_1 = 200\,\mu$m, and width of the smaller part of the trapezoid $w_0 = 50\,\mu$m; gap width d varied from 20 to $80\,\mu$m.

The conditions for excitation of a surface magnetostatic wave in micromagnetic modeling were established by applying external magnetic field H_0 along the y axis. The strength of external magnetic field H_0 was 1200 Oe.

When the problem of spin-wave signal transmission was being solved, absorbing layers with an exponentially increasing damping coefficient α were introduced at the boundaries of the structure (shaded regions in Fig. 1) in order to suppress the reflection of SWs from the boundaries of the calculation domain. The waveguide structure system under consideration had three ports. Microstrip antenna P_1 was positioned immediately after the damping region as a source of excitation of the spin-wave signal, and receiving antennas P_2 and P_3 were located at the output of the structure (see Fig. 1). The width of antennas P_1, P_2, and P_3

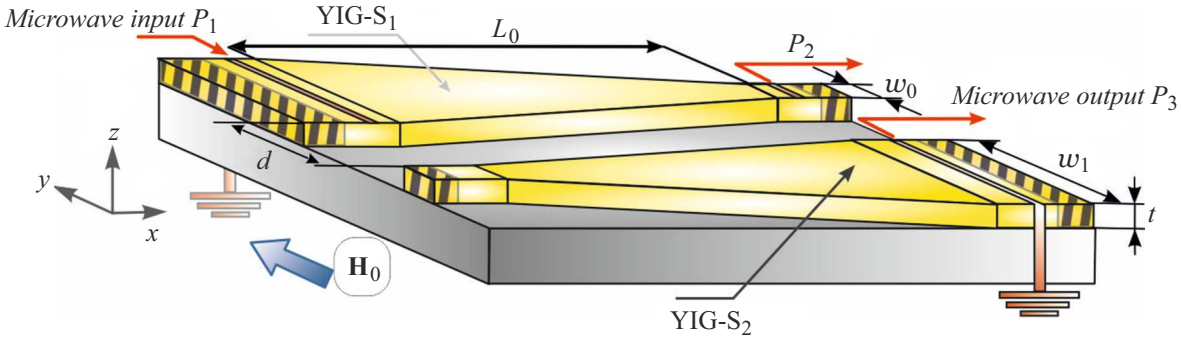

Figure 1. Image of the structure under study: a system of microwaveguides, which are fabricated based on a thin film of yttrium iron garnet, with linearly varying widths positioned laterally on a single substrate.

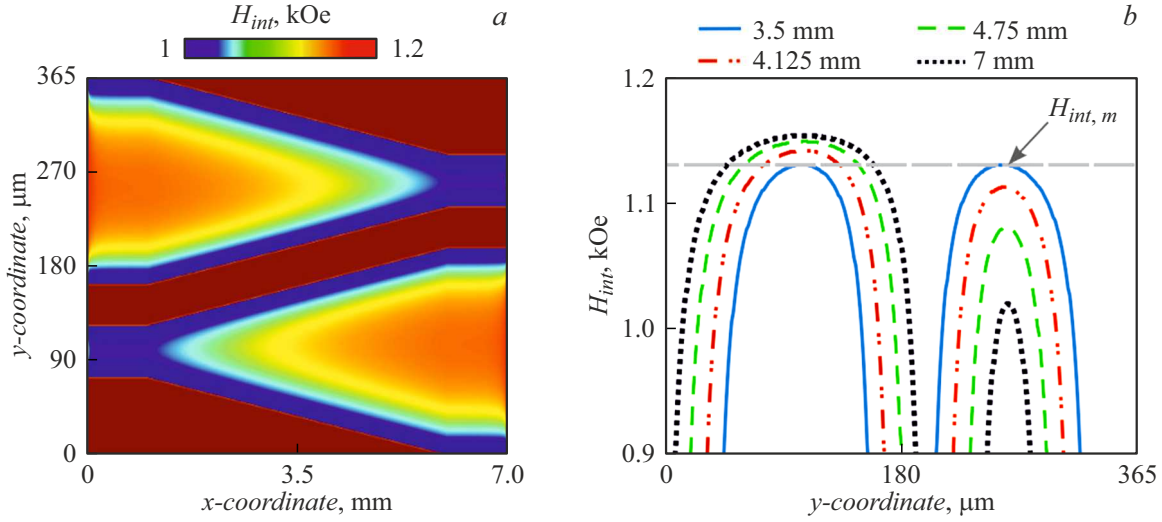

Figure 2. a — Map of the distribution of internal magnetic field H_{int} in a laterally coupled structure with linearly varying widths and gap $d = 40\,\mu$m. b — H_{int} distribution recorded at a fixed value of coordinate x: $x = 3.5$ mm (solid curve), 4.125 mm (dash-and-dot curve), 4.75 mm (dashed curve), and 7 mm (dotted curve).

was 30 μm. The length of antennas P_1 and P_3 was 200 μm, while antenna P_2 was 50 μm in length, which corresponds to the waveguide widths.

The study was carried out in the MuMax^3 software suite, where the modeled structure was mapped to a grid at the nodes of which the Landau–Lifshitz equation with Gilbert damping (LLG) [17,18] was solved numerically:

$$\frac{\partial \mathbf{M}}{\partial t} = \gamma\left[\mathbf{H}_{eff} \times \mathbf{M}\right] + \frac{\alpha}{M_s}\left[\mathbf{M} \times \frac{\partial \mathbf{M}}{\partial t}\right],$$

where $\mathbf{M}$ is the magnetization vector, $\alpha = 10^{-5}$ is the YIG film damping parameter, $\mathbf{H}_{eff} = \mathbf{H}_0 + \mathbf{H}_{demag} + \mathbf{H}_{ex} + \mathbf{H}_a$ is the effective magnetic field, $\mathbf{H}_0$ is the external magnetic field, $\mathbf{H}_{demag}$ is the demagnetization field, $\mathbf{H}_{ex}$ is the exchange field, $\mathbf{H}_a$ is the anisotropy field, and $\gamma = 2.8$ MHz/Oe is the gyromagnetic ratio.

The interaction between waveguides in the LLG equation was taken into account by calculating $\mathbf{H}_{eff}$ for the entire system, which includes all interactions. MuMax^3 directly solves the LLG equation numerically on a discrete grid with account for all interactions (exchange, dipole, Zeeman, etc.) without any preliminary approximations regarding the coupling strength. If the waveguides are far apart, the simulator indicates weak coupling. If they are close, strong coupling is revealed.

The static problem was considered first. The plotted distribution of internal magnetic fields H_{int} is shown in Fig. 2. Figure 2, a presents a map of the distribution of internal magnetic field H_{int} in two waveguides with smoothly varying widths and gap $d = 40\,\mu$m. It should be noted that H_{int} decreases with decreasing width of the waveguide channel. With the waveguides with linearly varying widths positioned laterally to each other, the magnitudes of internal magnetic field H_{int} in each waveguide at a fixed x-coordinate differ. Figure 2, b shows the H_{int} profiles along the x- coordinate that cover two waveguides with smoothly varying widths. It is fair to say that the only region where the H_{int} values for both waveguides are equal corresponds to $x = 3.5$ mm

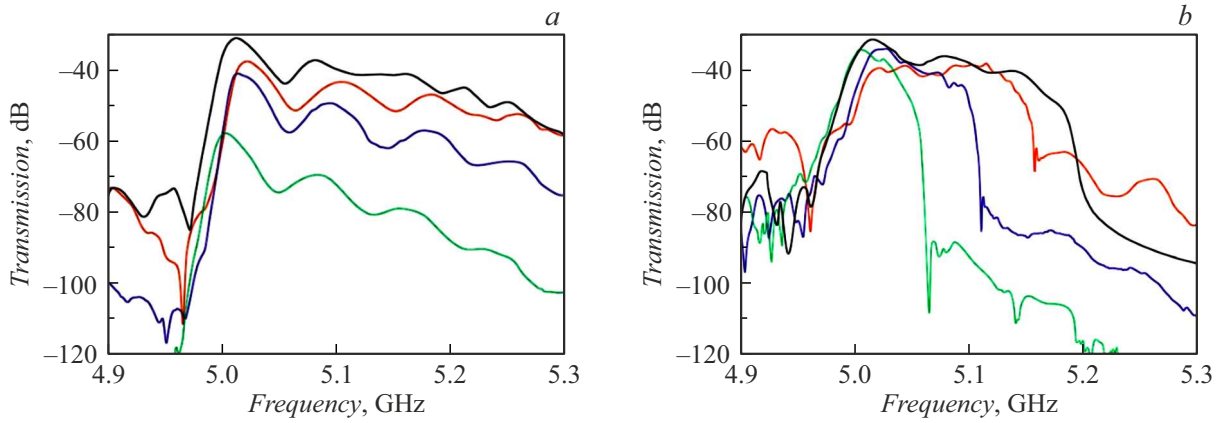

Figure 3. Amplitude-frequency responses for output ports P_2 (a) and port P_3 (b). The AFRs for gap $d = 20\,\mu$m (red curve), $40\,\mu$m (blue curve), and $80\,\mu$m (green curve) between the waveguides with a linearly varying width are indicated. The black curves correspond to AFRs for a single waveguide with a smoothly varying width recorded in the region with a waveguide width of 50 (a) and $200\,\mu$m (b). A color version of the figure is provided in the online version of the paper.

(marked with a gray dashed line and denoted as $H_{int,m}$). Shifting the probed region further along axis x, one may find a difference between the strengths of internal magnetic fields of two waveguides ΔH_{int} as large as ~ 150 Oe. A spin wave is transferred from one waveguide to another in the region where their widths are approximately equal, which is consistent with the theory of coupled modes [19]. According to this theory, when the magnitude of internal magnetic field H_{int} changes, the conditions for propagation of SWs are also altered, which leads to a shift of the dispersion curve and a change in the frequency range of their existence.

The configuration of waveguides with linearly varying widths and changing distance d between the waveguides was examined next. Figure 3 shows the amplitude-frequency responses (AFRs) obtained at output ports P_2 (a) and P_3 (b) and different gaps between the waveguides. The black curves correspond to the amplitude-frequency responses for a single waveguide with a smoothly varying width recorded in the region with a waveguide width of $50\,\mu$m (Fig. 3, a) and $200\,\mu$m (Fig. 3, b). The obtained AFRs for output port P_3 demonstrate that the frequency range grows narrower (with the high-frequency region being cut off) as the gap between waveguides with a linearly varying width gets wider. It should be noted that the higher the value of parameter d is, the stronger is the shift toward lower frequencies. At $d = 20$ and $80\,\mu$m. the difference between the cutoff frequencies is ~ 100 MHz. It should also be noted that the average transmission level for output port P_2 becomes lower as gap d gets wider.

Spatial maps of the SW intensity distribution were plotted for the observed AFR dips and the considered different values of parameter d (Fig. 4). At frequency $f = 5.068$ GHz (Fig. 4, a) and parameter $d = 20\,\mu$m, the spin wave is transferred into the lower planar waveguide. When parameter d increases to $40\,\mu$m at frequency $f = 5.062$ GHz (Fig. 4, b), the spin wave is also transferred into the lower planar waveguide, albeit with a lower power. When parameter d increases to $80\,\mu$m at frequency $f = 5.050$ GHz (Fig. 4, c), the regime of SW transfer into the lower planar waveguide is virtually indiscernible. With a further increase in d ($> 100\,\mu$m), the waveguides become isolated and cease to exert any influence on each other.

In all these three cases, re-emission of spin-wave power is seen in the SW intensity distribution maps at $x \sim 3.5$ mm, which is attributable to the fact that the magnitudes of internal magnetic fields H_{int} are equalized in this region. With an increase in parameter d, the intensity of the spin wave transferred into the adjacent waveguide decreases.

Thus, a system of laterally coupled waveguides with linearly varying widths was examined via numerical modeling. Amplitude-frequency responses and spatial maps of the SW intensity distribution were plotted to reveal the SW power redistribution regimes. The efficiency of SW transfer decreases as gap d between the microwaveguides grows wider. Owing to the effective signal re-emission at $x \sim 3.5$ mm and signal filtering with the high-frequency region being cut off, the examined structure may be used as a directional coupler and a microwave signal frequency filter in magnonic devices for data signal processing.

Funding

This study was carried out under the state assignment of the Ministry of Science and Higher Education of the Russian Federation (No. FZNS-2023-0012).

Conflict of interest

The authors declare that they have no conflict of interest.

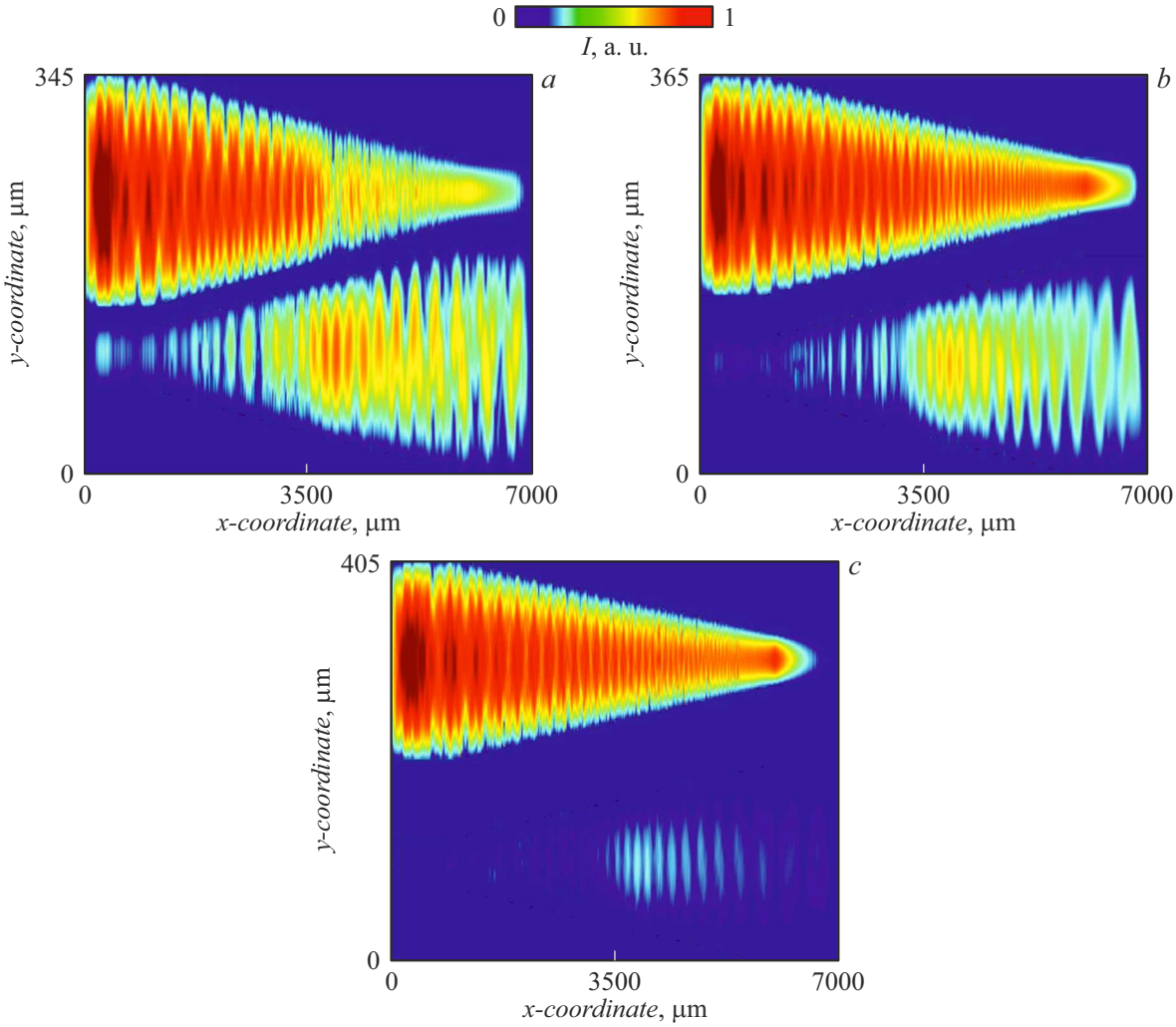

Figure 4. Spatial maps of the SW intensity distribution in a system of microwave guides positioned laterally on the same substrate at frequency $f_1 = 5.068$ GHz and $d = 20\,\mu$m (a), at $f_2 = 5.062$ GHz and $d = 40\,\mu$m (b), and at $f_3 = 5.050$ GHz and $d = 80\,\mu$m (c).

References

[1] S.A. Nikitov, D.V. Kalyabin, I.V. Lisenkov, A.N. Slavin, Yu.N. Barabanenkov, S.A. Osokin, A.V. Sadovnikov, E.N. Beginin, M.A. Morozova, Yu.P. Sharaevsky, Yu.A. Filimonov, Yu.V. Khivintsev, S.L. Vysotsky, V.K. Sakharov, E.S. Pavlov, Phys. Usp., **58** (10), 1002 (2015). DOI: 10.3367/UFNe.0185.201510m.1099.

[2] P. Schuddinck, F.M. Bufler, Y. Xiang, A. Farokhnejad, G. Mirabelli, A. Vandooren, B. Chehab, A. Gupta, C. Roda Neve, G. Hellings, J. Ryckaert, in *IEEE Symp. on VLSI Technology and Circuits* (*VLSI Technology and Circuits*) (IEEE, 2022), p. 365. DOI: 10.1109/VLSITechnologyandCir46769.2022.9830492

[3] A. Vandooren, N. Parihar, J. Franco, R. Loo, H. Arimura, R. Rodriguez, F. Sebaai, S. Iacovo, K. Vandersmissen, W. Li, G. Mannaert, D. Radisic, E. Rosseel, A.Y. Hikavyy, A. Jourdain, O. Mourey, G. Gaudin, S. Reboh, L.L. Van-Jodin, G. Besnard, C.R. Neve, B. Nguyen, I.P. Radu, E.D. Litta, N. Horiguchi, in *IEEE Symp. on VLSI Technology and Circuits (VLSI Technology and Circuits)* (IEEE, 2022), p. 330. DOI: 10.1109/VLSITechnologyandCir46769.2022.9830400

[4] G. Mirabelli, A. Vandooren, C. Roda Neve, V.V. Gonzalez, H. Mertens, A. Farokhnejad, P. Schuddinck, G. Murdoch, S.M. Salahuddin, O. Zografos, L. Ragnarsson, P. Weckx, Z. Tokei, G. Hellings, J. Ryckaert, Proc. SPIE, **12495**, 124951K (2023). DOI: 10.1117/12.2656456

[5] V. Demidov, S. Urazhdin, G. de Loubens, O. Klein, V. Cros, A. Anane, S. Demokritov, Phys. Rep., **673**, 1 (2017). DOI: 10.1016/j.physrep.2017.01.001

[6] V. Cherepanov, I. Kolokolov, V. L'vov, Phys. Rep., **229** (3), 81 (1993). DOI: 10.1016/0370-1573(93)90107-O

[7] S.L. Vysotsky, Yu.V. Khivintsev, V.K. Sakharov, G. Dudko, A. Kozhevnikov, S.A. Nikitov, N.N. Novitskii, A.I. Stognij, Yu.A. Filimonov, IEEE Magn. Lett., **8**, 3706104 (2017). DOI: 10.1109/LMAG.2017.2701787

[8] S. Sharko, A. Serokurova, N. Novitskii, V. Ketsko, A. Stognij, Ceramics, **6**, 1415 (2023). DOI: 10.3390/ceramics6030087

[9] C. Hauser, T. Richter, N. Homonnay, C. Eisenschmidt, M. Qaid, H. Deniz, D. Hesse, M. Sawicki, S.G. Ebbinghaus, G. Schmidt, Sci. Rep., **6**, 20827 (2016). DOI: 10.1038/srep20827

[10] A.V. Sadovnikov, C.S. Davies, V.V. Kruglyak, D.V. Romanenko, S.V. Grishin, E.N. Beginin, Y.P. Sharaevskii, S.A. Nikitov, Phys. Rev. B, **96**, 060401 (2017). DOI: 10.1103/PhysRevB.96.060401
[11] A.A. Martyshkin, C.S. Davies, A.V. Sadovnikov, Phys. Rev. Appl., **18**, 064093 (2022). DOI: 10.1103/PhysRevApplied.18.064093
[12] A.V. Sadovnikov, V.A. Gubanov, S.E. Sheshukova, Y.P. Sharaevskii, S.A. Nikitov, Phys. Rev. Appl., **9**, 051002 (2018). DOI: 10.1103/PhysRevApplied.9.051002
[13] V.E. Demidov, M.P. Kostylev, K. Rott, J. Münchenberger, G. Reiss, S.O. Demokritov, Appl. Phys. Lett., **99**, 082507 (2011). DOI: 10.1063/1.3631756
[14] D.V. Kalyabin, A.V. Sadovnikov, E.N. Beginin, S.A. Nikitov, J. Appl. Phys., **126**, 17 (2019). DOI: 10.1063/1.5099358
[15] A. Annenkov, S.V. Gerus, J. Commun. Technol. Electron., **41**, 196 (1996).
[16] A. Vansteenkiste, J. Leliaert, M. Dvornik, M. Helsen, F. Garcia-Sanchez, B.V. Waeyenberge, AIP Adv., **4**, 107133 (2014). DOI: 10.1063/1.4899186
[17] L. Landau, E. Lifshitz, Phys. Z. Sow., **8**, 153 (1935). DOI: 10.1016/b978-0-08-010586-4.50023-7
[18] T.L. Gilbert, J.M. Kelly, in *Conf. Magnetism and Magnetic Materials* (American Institute of Electrical Engineers, N.Y., 1955), p. 253–263.
[19] M.A. Morozova, N.D. Lobanov, O.V. Matveev, S.A. Nikitov, JETP Lett., **115** (12), 742 (2022). DOI: 10.1134/S0021364022600963.

Translated by D.Safin